DNN-based Outdoor NLOS Human Detection Using IEEE 802.11ac WLAN Signal

Ryo Takahashi*, Shigemi Ishida*, Akira Fukuda*, Tomoki Murakami‡, Shinya Otsuki‡
*ISEE, Kyushu University, Fukuoka, 819–0395, Japan
Email: {takahashi, ishida, fukuda}@f.ait.kyushu-u.ac.jp
‡Access Network Service Systems Laboratories, NTT Corporation, Kanagawa, 239–0847, Japan
Email: {tomoki.murakami.nm, shinya.otsuki.ma}@hco.ntt.co.jp

***Abstract*—Recently, WLAN-based wireless sensing technologies, which utilize WLAN devices widely used in many environments, have been focused because of their low deployment cost. We have presented an outdoor human detector using IEEE 802.11ac channel state information (CSI) for line-of-sight (LOS) scenarios in our previous work [1]. In this paper, we extend our previous work and present a CSI-based human detection system for outdoor non-line-of-sight (NLOS) scenarios. The key idea is to utilize CSI retrieved by multiple devices and extracted key features using principal component analysis (PCA) for sensing to avoid unstable detection performance. Experimental evaluations revealed that our human detection system for NLOS scenarios successfully located a human with an accuracy of 99.58 % using four WLAN stations.**

***Index Terms*—WLAN sensing, channel state information (CSI), outdoor human detection, principal component analysis (PCA).**

I. Introduction

Recently, wireless local area network (WLAN) based sensing technologies have been focused due to their low deployment cost. The WLAN sensing utilizes WLAN devices already installed in environments to monitor changes in a radio propagation environment by analyzing channel state information (CSI) defined in the WLAN standard [2]. While many papers have reported IEEE 802.11n CSI-based sensing technologies such as human localization and gesture recognition in an indoor environment [3]–[15], none of them have been adopted to outdoor environments. The number of multipaths becomes smaller in an outdoor environment, which puts difficulties in human location/activity recognition because of limited influence on wireless signals by human.

We have developed an IEEE 802.11ac CSI-based outdoor human detector [1]. The human detector retrieves 802.11ac CSI and perform multi-class classification using deep neural network (DNN) based supervised machine learning to locate the human in a sensing target area. The 802.11ac CSI, consists of amplitude and phase angle information for each WLAN orthogonal frequency division multiplexing (OFDM) subcarrier. We experimentally demonstrated that our human detector successfully located a human with an accuracy of 99.86 % in a line-of-sight (LOS) environment.

Our human detector, however, suffers from unstable detection performance depending on the location of CSI measuring stations. Moreover, we evaluated the human detector only in a LOS environment. The WLAN devices are often installed in non-line-of-sight (NLOS) environments in practical outdoor scenarios. Radio propagation model in an outdoor NLOS environment is completely different from the propagation model in an outdoor LOS environment, which highly affects the human detection performance. The NLOS environments increase the number of multipaths compared to LOS environments, which is not always true in outdoor environments.

We therefore present an outdoor human detection system for NLOS environments. The key idea is to utilize CSI from multiple CSI measuring stations and to extract key features for machine learning. CSI derived in outdoor environments includes much redundancy due to the small influence on different subcarriers from humans. We extract key features using principal component analysis (PCA) over CSI from multiple stations to increase training efficiency. Experimental evaluation in our university campus with four CSI measuring stations revealed that our outdoor NLOS human detection system successfully located human with an accuracy of 99.58 %.

The rest of the paper is organized as follows. Section II presents our outdoor NLOS human detection system, followed by experimental evaluations in Section III. Section IV summarizes the paper.

II. WLAN-based Outdoor NLOS Human Detection System

Figure 1 shows a system overview of the IEEE 802.11ac WLAN-based outdoor human detection system. The human detection system consists of data acquisition, pre-process, and machine learning block, which is the same as our previous system. We update the pre-process block with PCA to extract key features from CSI retrieved by multiple CSI measuring stations, as shown in Fig. 1b. The machine learning block performs supervised multi-class classification, which requires training prior to system use.

Each block is described in the following subsections.

A. Data Acquisition Block

The data acquisition block collects CSI from multiple WLAN stations named CSI measuring stations using a WLAN CSI monitoring system [16]. The data acquisition block consists of a WLAN access point (AP), CSI measuring stations, and CSI monitoring station, as shown in a left block in Fig. 1a. A WLAN AP and CSI measuring stations exchange CSI, i.e, beamforming report, using the IEEE 802.11ac sounding protocol. We install multiple CSI measuring stations in a sensing target area and collect CSI using a CSI monitoring station by capturing beamforming report messages. The

doi: 10.1109/SENSORS43011.2019.8956943

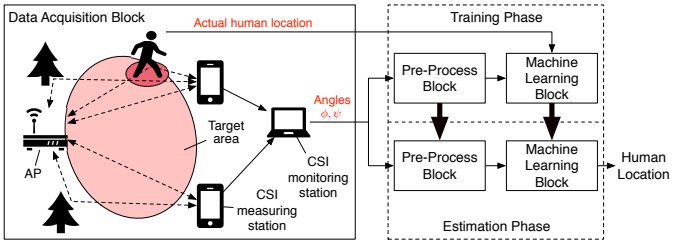

(a)

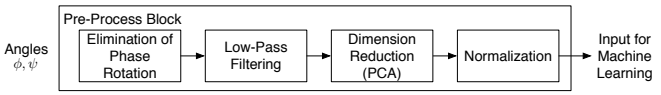

(b)

Fig. 1. System overview of WLAN-based outdoor NLOS human detection: (a) whole system and (b) structure of pre-process block.

captured CSI is compressed angle information $\phi \in [0, 2\pi)$ and $\psi \in [0, \pi/2)$ for each OFDM subcarrier [17]. ϕ and ψ indicate the difference of relative phase and amplitude between antennas, respectively.

B. Pre-Process Block

The pre-process block is responsible for four data processing: elimination of phase rotation, low-pass filtering, dimension reduction, and normalization.

The pre-process block first removes the influence of phase rotation in ϕ angle. The angle ϕ is in a range of $[0, 2\pi)$, implying that $\phi \simeq 0$ and $\phi \simeq 2\pi$ are the almost same angle. To handle such similarity of ϕ angles, we use $\sin\phi$ and $\cos\phi$ instead of ϕ as features for machine learning.

$\cos\phi$ and $\sin\phi$ data as well as ψ are then passed to a low-pass filtering process. The CSI data is highly sensitive to small environmental changes including sways of trees. We therefore apply a simple moving-average low-pass filter (LPF) over one-second CSI data.

To extract key features from CSI measured on multiple stations, PCA is applied to the low-pass-filtered angle information. CSI data includes much redundancy especially in outdoor environments because of the limited number of multipaths resulting in small CSI difference between subcarriers. We apply PCA and reduce the input dimension of a machine learning block, which increases training efficiency. The extracted component data is normalized by the min-max normalization algorithm and is passed to a machine learning block.

C. Machine Learning Block

The machine learning block locates a human by a supervised multi-class classifier. We don't limit the classification algorithm. In this paper, we implemented a deep neural network (DNN) based multi-class classifier as an example.

Figure 2 shows the architecture of the DNN we implemented. The DNN has two fully-connected hidden layers as well as input and output layers. The number of neurons in each hidden layer is set to be the number of principal components. We implemented the DNN with Keras/TensorFlow framework. Dropout [18] and Early Stopping [19] were employed in the model training.

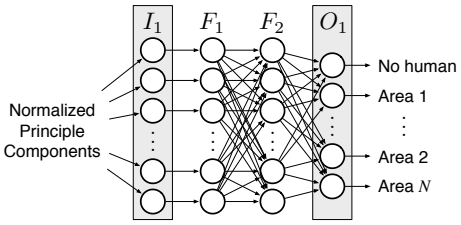

Fig. 2. Architecture of DNN for human detection

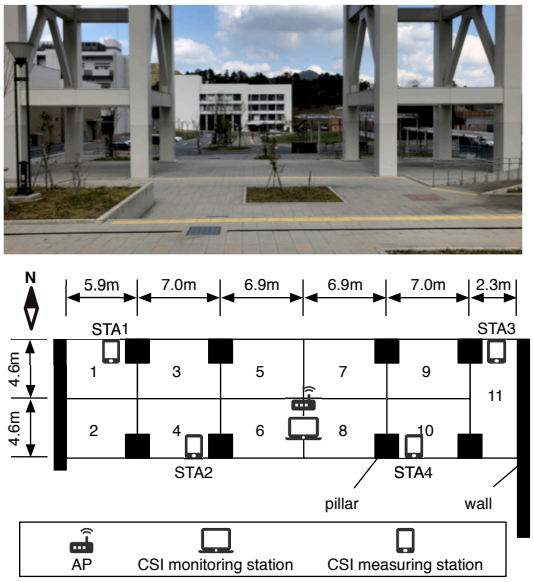

Fig. 3. Experiment environment

III. Evaluation

A. Experiment Setup

Figure 3 shows the experiment environment. To evaluate the performance in an NLOS environment, the experiment was conducted where there were multiple pillars and walls around a sensing target area. As shown in Fig. 3, four Galaxy S7 edge CSI measuring stations (STAs) were installed right behind the pillars. A testbed WLAN AP and Intel Compute Stick STK2m364CC CSI monitoring station were installed in the center of the sensing target area. 312 angle information ($= 6$ angles $\times$ 52 subcarriers) was collected with four antennas on AP and one antenna on each of the four STAs.

The target area was divided into 11 sub-areas labeled from `1` to `11`. The CSI data was collected at a sampling rate of 100 Hz for 60 seconds while a human was randomly walking in each area. We also collected CSI data with no human in the target area, labeled as `0`.

B. Detection Performance

We first evaluated the effect of multiple CSI measuring stations. We performed 10-fold leave-one-out cross validation with randomly shuffled data for 10 times. In each trial, nine-tenths data was used for training and one-tenth data was used for evaluation. The DNN in a machine learning block was

TABLE I
SENSING ACCURACY

CSI measuring stations	Accuracies w/o PCA
STA1	66.76 %
STA2	91.17 %
STA3	91.15 %
STA4	94.44 %
4 STAs	95.58 %

trained as a 12-class classifier with labels from `0` to `11`. We checked the capability of the system with data from the experiment. The model was re-trained in each cross-validation trial. In this evaluation, we omitted the PCA process.

Table I shows Accuracies of the detection performance using CSI derived from STA1–STA4 and 4 STAs. The "4 STAs" indicates that the detection system used CSI from all the four STAs. Table I demonstrates that the human detection using 4 STAs outperformed the detection using one CSI measuring station. Detection with single station exhibited unstable detection performance dependent on stations, while 4 STAs successfully removed the performance degradation.

C. PCA Performance

We next evaluated the effect of PCA in the detection performance. We evaluated detection performance using CSI derived from 4 STAs while changing the number of extracted principal components in a pre-process block. The detection performance was evaluated via 10-fold leave-one-out cross validation for three times for each number of principal components.

Figure 4 shows detection accuracy as a function of the number of principal components. Each CSI measuring station provides 468 dimensional CSI data after the elimination of phase rotation. The original dimension of 4-STA CSI data is therefore $468 \times 4 = 1872$. Figure 4 indicates that the accuracy increased as the number of principal components (PCs) increased and became maximum at 250 PCs. When the number of PCs was greater than 250, the detection accuracy slightly reduced as the number of PCs increased. The detection accuracy was 99.58 % when 250 PCs were used. Compared to the accuracies shown in Table I, we can confirm that PCA successfully improved the detection accuracy.

Figures 5 and 6 shows confusion matrices of area detection using 4-STA CSI without and with PCA, respectively. The figures show the detection results of 10-fold leave-one-out cross validation performed for 10 trials. A table in Fig. 5 indicates that areas 2, 4, and 8 were often mistakenly detected. Irrelevant CSI components for detecting the target object, i.e, a human, might have deteriorate the DNN model without PCA. With PCA, the detection performance was improved in these areas. With the limited number of principal components, we could emphasize the CSI changes affected by a human.

IV. CONCLUSION

In this paper, we presented a IEEE 802.11ac WLAN CSI-based outdoor human detection system for NLOS environments. We retrieve CSI, i.e, radio propagation environment information, from multiple WLAN devices and perform DNN-based multi-class classification to locate a human in a target area. We also employed PCA to extract key features for the machine learning to avoid unstable detection performance dependent on CSI measuring devices. We evaluated our detection system in an outdoor NLOS environment and demonstrated that the outdoor human detection system successfully located a human within 12 sub-areas with an accuracy of 99.58 %.

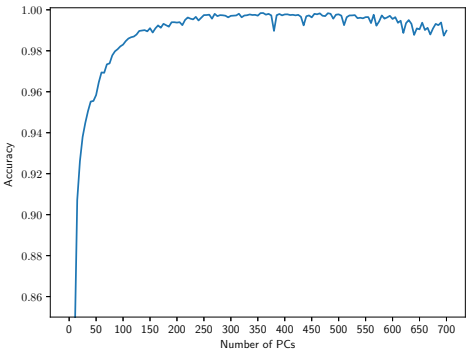

Fig. 4. Sensing accuracy for the number of principal component

Area	F-measure
0	99.95
1	95.47
2	90.37
3	96.77
4	91.81
5	98.62
6	97.48
7	97.74
8	90.69
9	96.19
10	97.96
11	92.52

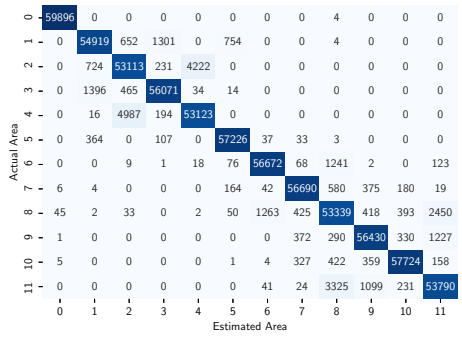

Fig. 5. Detection result using 4STAs without PCA

Area	F-measure
0	100
1	99.92
2	98.76
3	99.93
4	98.73
5	99.96
6	99.89
7	99.97
8	99.34
9	99.86
10	99.91
11	99.35

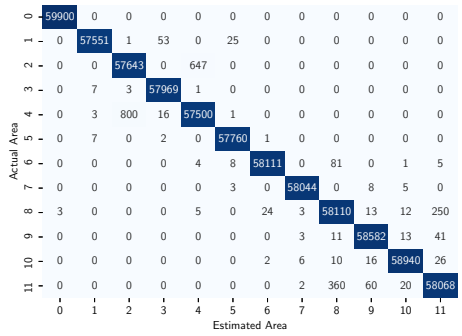

Fig. 6. Sensing result of 4STAs with PCA

ACKNOWLEDGMENT

This work was partially supported by JSPS KAKENHI Grant Number 15H05708 and JST ACT-I Grant Number JPMJPR18U2.

REFERENCES

[1] M. Miyazaki, S. Ishida, A. Fukuda *et al.*, "Initial attempt on outdoor human detection using IEEE 802.11ac WLAN signal," in *Proc. IEEE Sensors Aplications Symposium (SAS)*, Mar. 2019, pp. 1–6.

[2] IEEE Standards Association, "IEEE Std 802.11-2016, IEEE standard for local and metropolitan area networks — part 11: Wireless LAN medium access control (MAC) and physical layer (PHY) specifications," Jun. 2016, http://standards.ieee.org/.

[3] X. Zheng, J. Wang, L. Shangguan *et al.*, "Smokey: Ubiquitous smoking detection with commercial wifi infrastructures," in *Proc. IEEE Int. Conf. on Computer Communications (INFOCOM)*, Jul. 2016, pp. 1–9.

[4] X. Wang, C. Yang, and S. Mao, "TensorBeat: Tensor decomposition for monitoring multiperson breathing beats with commodity WiFi," vol. 9, no. 1, pp. 1–27, Sep. 2017, article No.8.

[5] S. Arshad, C. Feng, I. Elujide *et al.*, "SafeDrive-Fi: A multimodal and device free dangerous driving recognition system using WiFi," in *Proc. IEEE Int. Conf. on Communications (ICC)*, May 2018, pp. 1–6.

[6] H. Abdelnasser, M. Youssef, and K. A. Harras, "WiGest: A ubiquitous WiFi-based gesture recognition system," in *Proc. IEEE Int. Conf. on Computer Communications (INFOCOM)*, Apr.–May 2015, pp. 1–9.

[7] H. Abdelnasser, K. A. Harras, and M. Youssef, "A ubiquitous WiFi-based fine-grained gesture recognition system," *IEEE Trans. Mobile Comput.*, pp. 1–14, Nov. 2018, early access.

[8] C. Feng, S. Arshad, R. Yu *et al.*, "Evaluation and improvement of activity detection systems with recurrent neural network," in *Proc. IEEE Int. Conf. on Communications (ICC)*, May 2018, pp. 1–6.

[9] Z. Chen, L. Zhang, C. Jiang *et al.*, "WiFi CSI based passive human activity recognition using attention based BLSTM," *IEEE Trans. Mobile Comput.*, pp. 1–12, Oct. 2018, early access.

[10] Y. Wang, J. Liu, Y. Chen *et al.*, "E-eyes: Device-free location-oriented activity identification using fine-grained WiFi signatures," in *Proc. ACM MobiCom*, Sep. 2014, pp. 617–628.

[11] X. Wang, L. Gao, S. Mao *et al.*, "CSI-based fingerprinting for infoor localization: A deep learning approach," *IEEE Trans. Veh. Technol.*, vol. 66, no. 1, pp. 763–776, Jan. 2017.

[12] W. Wang, A. X. Liu, M. Shahzad *et al.*, "Understanding and modeling of WiFi signal based human activity recognition," in *Proc. ACM MobiCom*, Sep. 2015, pp. 65–76.

[13] W. Wang, A. X. Liu, M. Shahzad *et al.*, "Device-free human activity recognition using commercial WiFi devices," *IEEE J. Sel. Areas Commun.*, vol. 35, no. 5, pp. 1118–1131, May 2017.

[14] K. Ali, A. X. Liu, W. Wang *et al.*, "Keystroke recognition using WiFi signals," in *Proc. ACM MobiCom*, Sep. 2015, pp. 90–102.

[15] K. Ali, A. X. Liu, W. Wang *et al.*, "Recognizing keystrokes using WiFi devices," *IEEE J. Sel. Areas Commun.*, vol. 35, no. 5, pp. 1175–1190, May 2017.

[16] T. Murakami, M. Miyazaki, S. Ishida *et al.*, "Wireless LAN-based CSI monitoring system for object detection," vol. 7, no. 11, pp. 290:1–290:11, Nov. 2018.

[17] H. Yu and T. Kim, "Beamforming transmission in IEEE 802.11ac under time-varying channels," vol. 2014, pp. 1–11, Jul. 2014, article ID 920937.

[18] N. Srivastava, G. Hinton, A. Krizhevsky *et al.*, "Dropout: A simple way to prevent neural networks from overfitting," vol. 15, pp. 1929–1958, Jun. 2014.

[19] L. Prechelt, "Automatic early stopping using cross validation: quantifying the criteria," *Neural Networks*, vol. 11, no. 4, pp. 761–767, Jun. 1998.